Charge Transfer Equilibria Between Diamond and an Aqueous Oxygen Electrochemical Redox Couple

Vidhya Chakrapani, *et al.*

Science **318**, 1424 (2007);
DOI: 10.1126/science.1148841

Science (print ISSN 0036-8075; online ISSN 1095-9203) is published weekly, except the last week in December, by the American Association for the Advancement of Science, 1200 New York Avenue NW, Washington, DC 20005.

Charge Transfer Equilibria Between Diamond and an Aqueous Oxygen Electrochemical Redox Couple

Vidhya Chakrapani,[1] John C. Angus,[1]* Alfred B. Anderson,[1] Scott D. Wolter,[2] Brian R. Stoner,[3] Gamini U. Sumanasekera[4]

AUTHORS' SUMMARY

In 1989, Maurice Landstrass and K. V. Ravi observed a curious phenomenon—undoped diamond, known to be an exceedingly good insulator, showed substantial conductivity when exposed to air (*1*). The source of the conductivity has been uncertain and a matter of controversy since that time, which is surprising for such an important and long-studied material. Resolution of the problem is of inherent scientific interest and could be important for applications of diamond and in other contexts as well. Subsequent studies confirmed that the conductivity was confined to a near-surface region, carried by positive charge carriers (holes); and that the change occurred only when the diamond was covered with chemically bound hydrogen. Numerous proposals were made to explain the phenomenon; none has received wide acceptance. One recent proposal was that the effect occurred when electrons were transferred from the diamond to an electrochemical couple in an adsorbed water film (*2*). This proposal has received limited support, in part because it posited an adsorbed water film on an extremely hydrophobic substrate, and also because the energetics and dynamics of the proposed electrochemical couple were problematic.

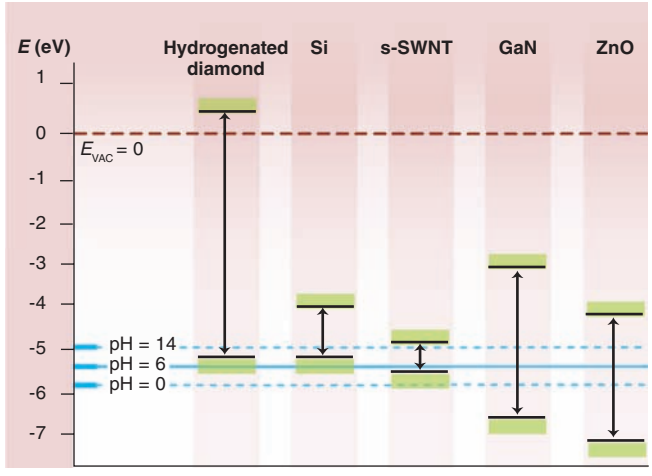

Electron energies of various solids. The vertical bars show the band gap. The continuous blue line is the electron energy of the oxygen couple in humid air (pH = 6); the lower dashed line is the value for pH = 0, the upper dashed line for pH = 14.

In this paper we describe a series of controlled experiments to explore this effect in which the presence of an aqueous phase is unambiguous. We hydrogenated diamond particles and measured the changes in pH and oxygen concentrations when the particles were added into aqueous solutions. These experiments show that electron exchange systematically occurs between diamond and the aqueous redox couple $O_2 + 4H^+ + 4e^- \rightleftharpoons 2H_2O$, which results in the consumption or formation of O_2. This electron exchange influences other properties—both the contact angle of water with the diamond surface and the amount and sign of the charge on diamond particles change in a predictable way by changing the extent of reaction that takes place. Adhesion of water to diamond is enhanced by electrostatic attraction after the charge transfer, which enhances the ability of water films to adsorb on otherwise hydrophobic surfaces.

These results imply that this process is a more general, unrecognized phenomenon that can influence a wide range of materials and processes. The key components are all derived from normal humid air: The water film provides both a medium for the electrochemical reaction as well as the O_2 and the H^+(the protons arise from acidity generated by CO_2 that is present in air). This means that the effect can occur whenever semiconductors or other solids are exposed to humid air.

The atmosphere thus provides a source of electrons whose electrochemical potential (Fermi energy) is fixed by the oxygen redox couple. If the atmosphere is in contact with a solid phase, electrons will transfer between the adsorbed water film and the solid in a direction that tends to bring the Fermi energy of the solid equal to that of the ambient film. The process is similar to that at a metal-semiconductor contact, except that a water film replaces the metal.

The electron energies of several solids and the oxygen redox couple in humid air are shown in the figure. In equilibrium in air, the couple fixes the Fermi energy of diamond at the top of the valence band, which generates positive charge carriers (holes). The energy range of the couple spans the band gap of semiconducting single-walled carbon nanotubes (s-SWNTs). For GaN, the electron potential of the redox couple lies near the states in the middle of the energy gap responsible for its ubiquitous "yellow band" luminescence (see the figure). Other experiments suggest that the conductivity of carbon nanotubes can be changed from that based on electrons to that based on holes, and that the intensity of luminescence from GaN can be modulated by changing the electrochemical potential of the ambient air (*3*).

Several caveats are in order. For the ambient air to fix the Fermi energy of a solid, there must be a large reservoir of reactants and facile reaction kinetics at the interface. The air provides quasi-infinite sources of O_2, H_2O, and CO_2; however, several factors can inhibit equilibration of the Fermi energies. An oxide layer, e.g., on silicon, or a thin film of adsorbed hydrocarbon can block electron exchange. The reduction of O_2 in the aqueous redox couple may require trace metallic impurities on the surface. Chemical ionization of oxidized surfaces, not involving electron transfer, and intrinsic conductivity in small–band gap semiconductors and metals can both mask the effect.

It is highly likely that the effects of electrochemically mediated charge transfer have remained unrecognized in many common situations. In this light, it will be of great interest to reexamine the literature on mechanical sliding friction and contact electrification, both of which depend in complex ways on relative humidity and impurities in the ambient air. Even more speculative is the possibility that certain animals and insects have evolved the capability of modulating the electrochemical potential in their feet to change the adhesive force to solid surfaces. Charge transfer to nanostructures not only can affect their properties, but also will vary with the size of the structure because of quantum confinement effects.

Summary References

1. M. I. Landstrass, K. V. Ravi, *Appl. Phys. Lett.* **55**, 975 (1989).
2. F. Maier, B. Riedel, J. Mantel, J. Ristein, L. Ley, *Phys. Rev. Lett.* **85**, 3472 (2000).
3. V. Chakrapani, J. C. Angus, A. B. Anderson, G. Sumanasekera, *Mater. Res. Soc. Symp. Proc.* **956**, paper J15-01 (2007).

FULL-LENGTH ARTICLE

Undoped, high-quality diamond is, under almost all circumstances, one of the best insulators known. However, diamond covered with chemically bound hydrogen shows a pronounced conductivity when exposed to air. This conductivity arises from positive-charge carriers (holes) and is confined to a narrow near-surface region. Although several explanations have been proposed, none has received wide acceptance, and the mechanism remains controversial. Here, we report the interactions of hydrogen-terminated, macroscopic diamonds and diamond powders with aqueous solutions of controlled pH and oxygen concentration. We show that electrons transfer between the diamond and an electrochemical reduction/oxidation couple involving oxygen. This charge transfer is responsible for the surface conductivity and also influences contact angles and zeta potentials. The effect is not confined to diamond and may play a previously unrecognized role in other disparate systems.

A highly unusual property of undoped, hydrogen-terminated diamond is the appearance of p-type surface conductivity when exposed to air (*1*). Sheet carrier concentration and mobility (*2*–*4*) have been measured and sensors and field effect transistors have been fabricated on the basis of this effect (*5*–*7*). Several mechanisms for the p-type conductivity have been proposed, including deep-level passivation by surface hydrogen (*1*), formation of shallow acceptors by subsurface hydrogen (*3*, *8*, *9*), oxidation by adsorbed gas molecules (*2*), and surface transfer doping to the H_2/H^+ redox couple in an adsorbed water layer (*10*, *11*). Larsson and co-workers presented a theoretical investigation of surface transfer doping to an acidic, adsorbed water film and gave a short review of other mechanisms (*12*, *13*). Recently Ristein (*14*) discussed surface transfer doping in the context of a new way of doping semiconductors, and Qi *et al.* (*15*) demonstrated surface transfer doping of diamond by tetrafluorotetracyanoquino-dimethane. However, despite much effort, no mechanism has received wide acceptance. Here, we present experimental evidence of electrochemically mediated charge transfer between diamond and macroscopic aqueous solutions. We also discuss the relevance of this effect for other material systems.

Rationale for experiments. The surface transfer doping mechanism involving the H_2/H^+ redox couple, as originally proposed (*10*, *11*), is in general agreement with the experimental observations of surface conductivity in diamond. However, it relies on the presence of an adsorbed water film on hydrophobic, hydrogen-terminated diamond. Adsorbed water films on solids exposed to humid atmospheres are common (*16*), but experimental evidence for water films on diamond is tenuous. In addition, the H_2/H^+ redox couple is unlikely to fix the potential in an adsorbed film because of the very low levels of H_2 in air. Finally, the absolute position of the H_2/H^+ couple is above the valence band maximum of hydrogen-terminated diamond that is exposed to air-saturated water and therefore unlikely to accept electrons from the valence band of diamond.

In the light of the above, experiments testing the surface transfer doping mechanism when the presence of an aqueous phase is unambiguous are attractive. Furthermore, experiments in which the dissolved oxygen concentration can be controlled and measured can distinguish between the H_2/H^+ redox couple (*10*, *11*) and the O_2 couple suggested by Foord *et al.* (*17*) and Chakrapani *et al.* (*18*). Because fluorinated and oxidized diamond have similar electron affinities, but very different surface chemistries, we opted to explore fluorinated as well as oxidized and hydrogenated samples.

The sheet concentration of holes in diamond exposed to moist air has been estimated to be on the order of 10^{12} to 10^{13} cm^{-2} (*2*, *3*). If this charge arises from electrochemical transfer doping, a straightforward calculation shows that addition of high–surface area diamond powder to small, but macroscopic, amounts of aqueous solution will produce measurable changes in pH and in dissolved oxygen concentration. Furthermore, the direction of these changes will differ depending on whether the Fermi level of the diamond is above or below the electrochemical potential of the aqueous solution.

Electron transfer between diamond and aqueous solutions should produce other macroscopic effects as well. The contact angle of aqueous solutions with diamond should decrease at low pH because of increased electrostatic attraction between the positive accumulation layer in the diamond and compensating negative ions in the adjacent solution. The sign of the zeta potential, which is related to the sign of the net charge on a particle, should vary in a similar systematic way with pH, i.e., greater positive surface charge at lower pH.

Electrochemical potentials and band line-up. According to the electrochemical transfer doping model, a p-type accumulation layer forms in diamond when the Fermi level of the diamond is higher than the electrochemical potential, μ_e, of an adsorbed water layer on the diamond surface (*10*, *11*). Electrons transfer from the diamond to the water layer, resulting in a positive space charge layer in the diamond and compensating anions in the water layer. The electrochemical potential of the film is determined by electrochemical redox couples involving dissolved oxygen in equilibrium with air (*17*, *18*).

$$O_2 + 4H^+ + 4e^- \rightleftharpoons 2H_2O \quad \text{dominates at acidic conditions} \qquad (1)$$

$$O_2 + 2H_2O + 4e^- \rightleftharpoons 4OH^- \quad \text{dominates at basic conditions} \qquad (2)$$

The reactions in Eq. 1 and 2 are not independent, but are related by the water equilibrium, Eq. 3.

$$H_2O \rightleftharpoons H^+ + OH^- \qquad (3)$$

Although electrons are not present as separate entities in the aqueous phase, their electrochemical potential, μ_e, is well defined and is given by the Nernst equation. The reactions in Eqs. 1 and 2 have expressions for μ_e given, respectively, in Eqs. 4 and 5.

$$\mu_e(\text{eV}) = -4.44 + (-1)(+1.229) + \frac{0.0592}{4}[4\text{pH} - \log_{10}(p_{O_2})] \qquad (4)$$

$$\mu_e(\text{eV}) = -4.44 + (-1)(+0.401) - \frac{0.0592}{4}[4\text{pOH} + \log_{10}(p_{O_2})] \qquad (5)$$

Here, μ_e (eV) is referred to the vacuum level, the activity of H_2O is assumed to be unity, the ideal gas approximation is used, the temperature $T = 298$ K, and the partial pressure of O_2, p_{O_2}, is in bar. The electrochemical potential of electrons in the standard hydrogen electrode (SHE) relative to the vacuum level is $\mu_{e(SHE)} = -4.44$eV (*19*, *20*). The standard electrode potentials of the reactions in Eqs. 1 and 2 are +1.229 V and +0.401 V versus SHE, respectively (*21*). The relation between pH and pOH is simply pH + pOH = 14.

Mott-Schottky measurements (*22*) and theoretical considerations (*23*) indicate that the electron affinity, EA, of hydrogen-terminated diamond in contact with water or moist air is approximately −0.30 eV, which is 1 eV more positive than the value obtained in vacuum (*24*). Because the diamond band gap is 5.5 eV, this shift places the top of the diamond valence band at approximately −5.2 eV. This estimate was used to give the position of the band edges of diamond in Fig. 1. Also shown in Fig. 1 are the electrochemical potentials for the oxygen redox couple calculated from Eqs. 4 and 5 for $p_{O_2} = 0.21$ bar and pH = 0 and pH = 14. These energies, −5.66 eV and −4.83 eV, respectively, straddle the estimated position of the valence band maximum of diamond.

The band line-up shown in Fig. 1 is for hydrogen-terminated diamond in contact with an aqueous phase. Oxygen and fluorine are both

[1]Case Western Reserve University, Cleveland, OH 44106, USA. [2]Duke University, Raleigh-Durham, NC 27708, USA. [3]Research Triangle Institute, Research Triangle Park, NC 27709, USA. [4]University of Louisville, Louisville, KY 40291, USA.

*To whom correspondence should be addressed. E-mail: john.angus@case.edu

more electronegative than carbon in contrast to hydrogen, which is more electropositive than carbon. Therefore, surface termination with either oxygen or fluorine induces a surface dipole that will increase the electron affinity, opposite to the effect in hydrogen-terminated diamond. The electron affinity of an oxidized diamond surface is about 1 eV more positive than hydrogenated surfaces (*24*, *25*), and the effect of fluorine is expected to be similar. This lowering of the diamond energy bands by ≈ 1 eV places the valence band maximum at $E \approx -6.2$ eV, below the electrochemical potential of the aqueous phase at all pH's.

Electrochemically mediated charge transfer. Water in equilibrium with air has a pH ≈ 6 from the naturally occurring CO_2 in the air, which corresponds to an electrochemical potential of $\mu_e \approx -5.3$ eV from Eq. 4. Lowering the pH lowers μ_e. Therefore, addition of hydrogenated diamond powder equilibrated with moist air to a solution with pH < 6 leads to $\mu_e(\text{dia}) > \mu_e(\text{aq})$, and electrons transfer from the diamond to the solution until $\mu_e(\text{dia}) = \mu_e(\text{aq})$. The reaction in Eq. 1 proceeds in the forward direction, which results in consumption of protons. However, when diamond powder equilibrated with moist air is brought in contact with a basic solution, $\mu_e(\text{dia}) < \mu_e(\text{aq})$; electrons transfer from the solution into the diamond, which drives the reaction in Eq. 2 in the reverse direction. Hydroxyl ions are consumed and the solution becomes more acidic. If these are the only processes taking place at the interface, the protons consumed plus the hydroxyl ions formed are equal to the number of electrons transferred from the diamond to the solution. Reduction in the concentration of electrochemical acceptors, i.e., the dissolved oxygen, should decrease the amount of electron transfer from the diamond and suppress the changes of pH of the solution.

The overall stoichiometry of the electrochemically mediated charge transfer at moderate pH can be written as Eq. 6 (*18*):

$$4(e^-h^+)_{\text{dia}} + O_{2,\text{air}} + 2H_2O_{\text{air}} + 4CO_{2,\text{air}} \rightleftharpoons 4h^+_{\text{dia}} + 4HCO^-_{3,\text{aq}} \quad (6)$$

Equation 6 describes the situation when the acidity is generated by atmospheric CO_2. In this case, the counterions in the aqueous phase are dominantly HCO_3^-. The type of counterion will depend on the ambient. For example, in the presence of HCl vapors, the counterions will be predominantly Cl^-.

We note that the electron affinity of the aqueous oxygen redox couple is much greater than that of molecular oxygen and other gas-phase oxidants in the absence of water. For example, the electron affinity of O_2 is EA = +0.451 eV (*26*), which places the energy at $E = -EA = -0.451$ eV, far above the energy of the oxygen redox couple at any pH (Fig. 1). The electron affinities of other highly oxidizing gas-phase species, e.g., NO_2, O_3, and F, are, respectively, 2.273, 2.103, and 3.4 eV (*26*) and thus are also not sufficient to directly oxidize diamond. Therefore, direct electron transfer from diamond to gas-phase species in the absence of water is thermodynamically improbable.

Titration of diamond powder. Natural diamond powder with a nominal size range of 0.5 to 1.0 μm was purchased from Advanced Abrasives Corp. The as-purchased powder was oxidized and was therefore hydrogenated at 700°C for 4 hours in a 2.45-GHz microwave plasma reactor supporting a hydrogen plasma at 750 W, at a gas flow rate of 196 standard cubic centimeters per minute and pressure of 35 torr. The powder was cooled in hydrogen gas to room temperature, stirred, and the process then repeated two times to ensure good hydrogen coverage. X-ray photoelectron spectroscopy (XPS) analysis indicated that the surface oxygen concentration was lowered from 8.5 to 1.4% by this process. Because the samples were transferred in air, the bulk of the residual oxygen likely arose from physically adsorbed species.

Diamond powder was fluorinated in a planar, inductively coupled 13.56-MHz plasma reactor at 800 W with a dc bias of –307 V. A source gas of SF_6 at 25 sccm was used to maintain a pressure of 0.035 torr for 10 min. The substrate temperature was maintained at 20°C. Subsequent XPS analysis of the powder showed both fluorine and oxygen on the surface in approximately a 5/1 atomic ratio.

In all of the titration experiments with diamond powder, 1 g of powder was added to 20 ml of solution. The solution was stirred continuously before and after addition of the diamond powder. The pH and dissolved oxygen concentration measurements were made with an Accumet XL60 meter. Analytical-grade chemicals (HCl, NaOH, and $NaHSO_3$) were used in all experiments, and solutions were filtered through a 0.1-μm filter before use. Air-saturated water was used for most experiments. In some cases, the dissolved oxygen concentration was reduced by bubbling nitrogen through the solution for 4 hours and then

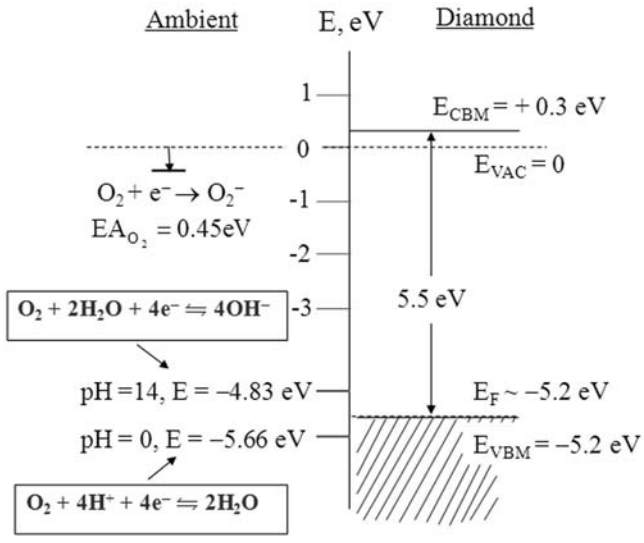

Fig. 1. Estimated band lineup of hydrogen-terminated diamond in contact with an aqueous solution. The electrochemical potentials of the oxygen redox couple are shown at pH = 0 and pH = 14. The electron affinity of gaseous O_2 is also shown (E = – EA = – 0.451 eV).

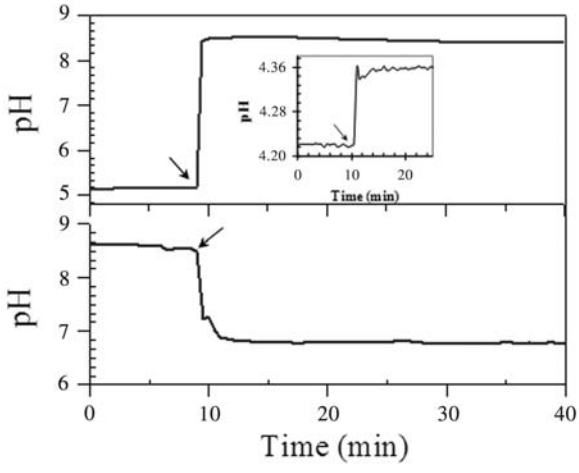

Fig. 2. Changes in pH upon addition of 1 g of hydrogen-terminated natural diamond powder, equilibrated with air, to separate 20-ml aqueous solutions with pH = 5.2 and pH = 8.5. The arrows indicate the point where the diamond powder was added. For the former, μ_e (dia) > μ_e (aq) and electrons transfer into the liquid, thereby consuming protons and raising the pH. For the latter, μ_e (dia) < μ_e (aq), and electrons transfer out of the solution, lowering the pH. The inset shows the result when hydrogen-terminated diamond powder is added to a solution deoxygenated with N_2 and $NaHSO_3$. Note the expanded vertical scale.

adding sodium bisulfite up to a concentration of 0.5 M. The original dissolved oxygen concentration of air-saturated water was ~7 mg/liter; the concentration after the nitrogen purge and bisulfite treatment was less than the sensitivity of the dissolved oxygen probe (0.01 mg/liter). For experiments with sodium bisulfite, the chamber was closed to isolate the solution from the open air, and nitrogen was continuously purged through the chamber.

Figure 2 shows the changes in pH when 1 g of hydrogenated diamond powder is added separately to 20 ml of air-saturated aqueous solutions, one at pH = 5.2 and the other at pH = 8.5. The pH increases upon addition of the hydrogenated diamond to the acidic solution and decreases upon addition of the diamond powder to the basic solution. These changes are in the expected directions described above. The inset in Fig. 2 shows the change in pH when hydrogenated diamond powder is added to a solution that has been deoxygenated with N_2 and $NaHSO_3$. The change in pH is very small (note the magnified vertical scale). This result indicates that dissolved oxygen is necessary for charge transfer to take place.

Figure 3A shows a titration curve obtained by addition of 1 g of diamond powder equilibrated with room air to 20-ml solutions of known pH. The ordinate is the number of electrons, ΔN_{e^-}, transferred into the water and is given by Eq. 7,

$$\Delta N_{e^-} = \Delta N_{OH^-} - \Delta N_{H^+} = N_{AV} V_{H_2O} \times \{10^{-14}(10^{pH_f} - 10^{pH_i}) - (10^{-pH_f} - 10^{-pH_i})\} \quad (7)$$

where N_{AV} is Avogadro's number, ΔN_{H^+} and ΔN_{OH^-} are the changes in number of H^+ and OH^- ions respectively, V_{H_2O} is the volume of water in liters, and pH_i and pH_f are the initial and final pH of the solution. At high pH, the first term dominates; at low pH, the second term dominates. In the flat portion of the titration curve, both protons and hydroxyl ions are present in low concentrations, and the transfer of a small number of electrons leads to large changes in pH.

The crossover point in Fig. 3, A and B, is where the electrochemical potential of the solution is equal to the Fermi level of the original diamond equilibrated with air. The electrochemical potential of the solution at this point is a direct measure of the Fermi level of diamond equilibrated with room air. The crossover point is most easily seen in Fig. 3B and is estimated to occur at pH = 6.1, which from Eq. 4 corresponds to an electron chemical potential of $\mu_e = -5.3$ eV. This value is in close agreement with independent Mott-Schottky and Kelvin probe measurements that show $\mu_e = -5.2$ eV (*22*, *27*) for diamond in equilibrium with aqueous solutions in air.

We estimated the change in the concentration of dissolved oxygen upon addition of diamond powder by using an electrochemical biochemical oxygen demand (BOD) probe consisting of a FEP Teflon membrane covering a gold and silver electrode. When hydrogenated diamond powder, previously equilibrated with room air, is added to an acidic solution, $\mu_e(\text{dia}) > \mu_e(\text{aq})$; electrons transfer into the solution and the concentration of dissolved oxygen decreases due to the reaction in Eq. 1, which proceeds in the forward direction. When hydrogenated diamond powder is added to a basic solution, $\mu_e(\text{dia}) < \mu_e(\text{aq})$, and the concentration of dissolved oxygen increases. In this latter case electrons leave the solution, driving the reaction in Eq. 2 in the reverse direction, thus increasing the concentration of dissolved oxygen. The results are summarized in Table 1. In both cases, the change in dissolved oxygen concentration is in the expected direction. Furthermore, the estimated change in number of moles of dissolved oxygen agrees with the change in number of molecules of protons and hydroxyl ions calculated from the pH change within the expected error of the oxygen measurement.

Zeta potential measurements. Zeta potentials are obtained by measurement of the electrophoretic velocity of dispersed solids in a liquid. The magnitude and sign of the zeta potential depend on the net amount and sign of the charge within the shear boundary separating the mobile liquid from the stagnant layer near the solid surface. A positive zeta potential indicates a net positive charge within the shear boundary; a negative zeta potential indicates a net negative charge (*28*). Here we use measurements of the zeta potential as confirmation of the direction of electron transfer between diamond powder and water.

We performed zeta potential measurements with a ZETAMASTER-S using 1-μm nominal-size natural diamond powder purchased from SJK-5, Kay Industrial Diamond Corp. Hydrogenation and fluorination of the powder were performed as described earlier. The diamond powder was equilibrated with room air before the zeta potential measurements were made.

From Fig. 4 it is evident that hydrogen-terminated diamond powder shows a positive zeta potential at all pH values less than 7. This result is consistent with electron transfer from the diamond, which increases with decreasing pH as predicted by the transfer doping model. The slightly negative zeta potentials for the hydrogen-terminated diamond at pH > 8 are consistent with a low concentration of residual oxygen-containing surface functional groups on the surface compared to the nonhydrogenated samples.

The zeta potentials for both oxidized and fluorinated diamond powder differ markedly

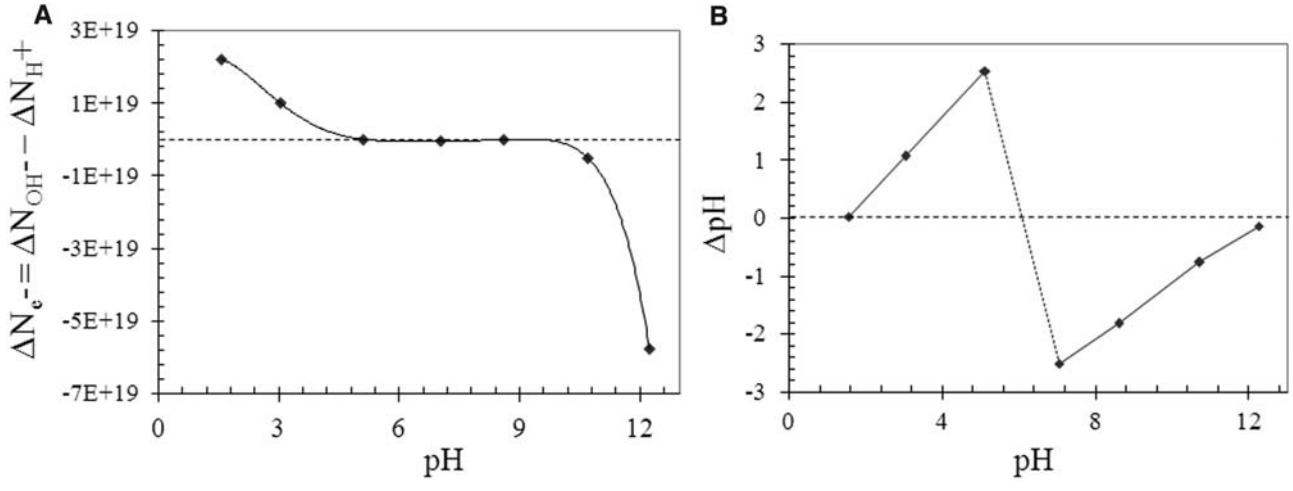

Fig. 3. (**A**) Number of electrons transferred from the diamond upon addition of 1 g of hydrogen-terminated natural diamond powder equilibrated in air to 20-ml aqueous solutions of varying initial pH. The crossover point is where the Fermi level of the diamond equals the chemical potential of electrons in equilibrium with the electrochemical couple. (**B**) Change of pH upon addition of 1 g of hydrogen-terminated natural diamond powder equilibrated in air to 20-ml solutions of varying initial pH.

from those of the hydrogen-terminated powder. The potentials for these samples are similar in magnitude and negative at all pH values greater than 1. The negative charge can arise either from transfer of electrons to the diamond or ionization of residual oxygen-containing functional groups on the surface, e.g., carboxylic acids and hydroxyl radicals. The similarity of the results for the oxidized and fluorinated samples indicates that the charging process is similar despite the different surface chemistry of the two types of samples.

Contact angle measurements. Advancing contact angles on hydrogen-terminated, 3-mm diamond macles in solutions of different pH were determined. Macles are natural, triangular, unpolished, twinned single crystals of diamond. We measured the contact angles on the (111) facets of these crystals by the Wilhelmy plate technique (*29*) using a KRÜSS K100 Processor Tensiometer. The diamond samples were first hydrogenated under conditions described above for diamond powders for a period of 2 hours. After hydrogenation, they were cleaned ultrasonically in Milli-Q water for 10 min and dried under flowing N_2.

The macles were suspended by a corner from the arm of the electrobalance and immersed in the solution at a constant rate of 3 mm/min while we measured the force on the sample due to wetting. The contact angle was calculated from the measured force, wetted length of the sample, and the surface tension of the solution, γ_{LV} (*29*). Extrapolation of the results to zero immersion depth eliminated the effect of variation of the length of the wetted perimeter. The surface tension of the solution was measured with a roughened platinum plate, which is wetted with a contact angle of virtually 0°. By measuring the force acting on the plate when immersed in the solution, we calculated γ_{LV}.

The advancing contact angles of a hydrogen-terminated diamond macle in contact with aqueous solutions of varied pH and dissolved oxygen content are shown in Fig. 5A. We attribute the decrease of the contact angle at low pH to the electrostatic attraction between the positive space charge layer in the diamond and the compensating anions in the aqueous phase (*18*). The solvated anions provide a mechanism for binding a water film to the hydrogen-terminated, hydrophobic diamond surface.

Reduction in the concentration of electrochemical acceptors, i.e., the dissolved oxygen, should decrease the electron transfer from the diamond and reduce the effect of pH on contact angle. First, we lowered the dissolved oxygen concentration in the water by bubbling nitrogen through the solution. Further removal of dissolved oxygen was achieved by reduction with sodium bisulfite (*30*). From Fig. 5A, it is clear that the contact angle increased as the concentration of dissolved oxygen decreased. Furthermore, the dependence of contact angle on pH essentially disappeared after the addition of excess sodium bisulfite, which reduces the dissolved oxygen concentration to very low levels.

The work of adhesion, W_{ad}, which is the energy required to separate the liquid and solid

Table 1. Summary of results showing changes in the concentration of dissolved oxygen (DO) and pH with the addition of 1 g of hydrogenated natural diamond powder equilibrated with air to 20 ml of solution. The change in number of ions of H^+ and OH^- is from Eq. 7.

	Steady-state value before addition	Steady-state value after addition	Change in no. of molecules	No. of e^- transferred
DO (mg/liter)	7.8	7.3	1.9×10^{17} of O_2	$+7.6 \times 10^{17}$
pH	4.1	5.3	8.9×10^{17} of H^+ and OH^-	$+8.9 \times 10^{17}$
DO (mg/liter)	6.9	7.5	2.3×10^{17} of O_2	-9.2×10^{17}
pH	7.3	4.4	4.8×10^{17} of H^+ and OH^-	-4.8×10^{17}

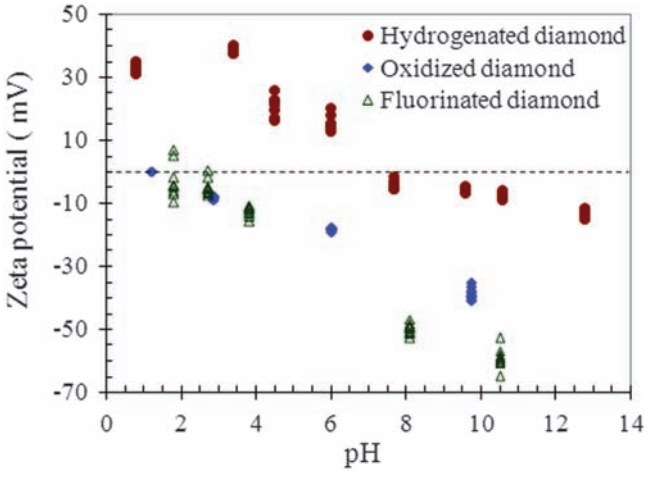

Fig. 4. Zeta potential as a function of pH for hydrogenated, oxidized, and fluorinated natural diamond powder. Hydrogen-terminated diamond shows a positive zeta potential (positive surface charge) at pH < 7. Fluorinated and oxidized diamond powders show negative zeta potentials (negative surface charge) at all pH's.

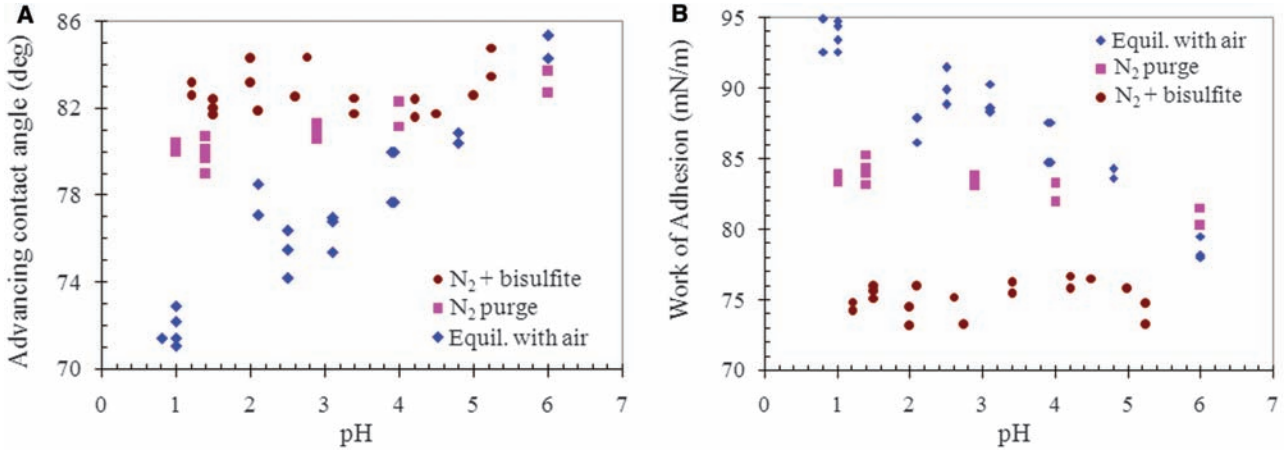

Fig. 5. (**A**) Advancing contact angles on a (111) surface of a hydrogen-terminated diamond macle as a function of pH. Experiments were performed with water in equilibrium with air, water purged with N_2, and water purged with N_2 and treated with $NaHSO_3$. (**B**) Changes in the work of adhesion calculated from the contact angles. Experiments were performed with water in equilibrium with air, water purged with N_2, and water purged with N_2 and treated with $NaHSO_3$.

phases, is related to the contact angle, θ, through the Young-Dupre equation (*16*), (Eq. 8).

$$W_{ad} = \gamma_{LV}(1 + \cos\theta) \quad (8)$$

Figure 5B shows the work of adhesion as a function of pH of the solution. Higher work of adhesion is found at lower pH for air-saturated solutions; the work of adhesion for deoxygenated solutions is reduced and is independent of pH, as expected.

Role of oxygen. Our results support the surface transfer doping mechanism (*10*, *11*), but are consistent with charge transfer between diamond and an electrochemical redox couple involving O_2 in the adjacent water phase as suggested by Foord *et al.* (*17*) and Chakrapani *et al.* (*18*), rather than the H_2/H^+ couple as originally proposed.

Fixing the electrochemical potential and pinning the Fermi level in the diamond require facile electron transport between the diamond and the adjacent aqueous phase. The redox reactions (Eqs. 1 and 2) must be sufficiently rapid to permit measurable charge exchange within the time of the measurements. The relatively large concentration of O_2 (compared to H_2) in air-equilibrated water facilitates the reaction kinetics of Eqs. 1 and 2. The reduction of O_2 in the aqueous redox couple may require trace metallic impurities on the surface to proceed at appreciable rates. Furthermore, an adsorbed organic film can displace the aqueous phase and suppress the effect (*18*). The use of epoxy resins to insulate electrical contacts may provide such a barrier.

We emphasize that under certain conditions, other processes not involving electron transfer may take place. For example, surface field effect devices have been constructed with the use of induced charge (*7*). Also, on an oxidized diamond surface, functional groups such as carboxylic acid and hydroxyl can ionize (Eqs. 9, 10).

$$(\text{dia})\text{-COOH} \rightleftharpoons (\text{dia})\text{-COO}^- + \text{H}^+ \quad (9)$$

$$(\text{dia})\text{-OH} \rightleftharpoons (\text{dia})\text{-O}^- + \text{H}^+ \quad (10)$$

The total number of sites on a (111) diamond surface is ~10^{15} cm^{-2}. Therefore, even a 1% surface coverage with ionizable sites can mask the effects of transfer doping, which gives rise to sheet charge densities of ~10^{12} to 10^{13} cm^{-2} (*2*–*4*).

Because the reactions in Eqs. 9 and 10 do not involve electrons, their equilibria do not depend on the chemical potential of electrons, μ_e. However, these reactions do involve protons, so their equilibria depend on the chemical potential of protons, i.e., on pH. The reaction in Eq. 9 will proceed to the right if the pH of the aqueous phase meets the condition pH > pK_a ≈ 4; similarly, the reaction in Eq. 10 will proceed if pH > pK_a ≈ 10. Here pK_a is the acid dissociation constant of the functional groups. If these conditions are met, protons transfer into the solution, lowering the pH. This effect is illustrated in Fig. 6. The pH of a solution, initially at pH ≈ 5, decreases upon addition of oxidized diamond powder. In contrast, when hydrogenated diamond is added to a solution with pH ≈ 5, surface transfer doping causes the pH to increase.

All of the experiments have been performed with natural type IA diamond, which contains appreciable quantities of nitrogen. However, the nitrogen in natural diamond is present as aggregates and, as such, does not provide active donor centers (*31*, *32*). In contrast, in type Ib synthetic diamond, single substitutional nitrogen atoms are present, which have a donor level 1.6 eV below the conduction band minimum (*33*). If present, these donor centers can ionize and compensate holes generated by electron transfer to the aqueous phase (*34*). In this situation, positively charged donor sites and holes are charge-balanced by excess anions in the aqueous phase. Because all of our experiments were conducted with type IA diamond, which has negligible substitutional nitrogen, compensation by nitrogen donors does not occur. Indeed, we found that the surface conductance of the type IA diamond is four orders of magnitude greater than the conductance of type Ib, 2 × 2 mm (100) synthetic diamond crystals (Sumitomo, HTHP).

Electrochemically mediated charge transfer in other material systems. Electrochemically mediated transfer doping was first noted in diamond (*1*) because the effect on conductivity is so striking. However, the phenomenon should occur in many other systems if the band line-up is appropriate. Furthermore, the electrostatic attraction between the resulting space charge layer in the solid and the compensating ions in the adsorbed film will enhance the formation of adsorbed water films.

The electron affinity of semiconducting single-walled nanotubes (SWNTs) has been reported to be 4.8 eV (*35*). Also, SWNTs have a band gap of 0.4 to 0.6 eV and a work function of 4.8 to 5.1 eV (*36*, *37*). These values place the Fermi level above the electrochemical potential of the aqueous redox couple (Eq. 1) for air-saturated water, which is ~ −5.3 eV. Hence, when SWNTs are exposed to humid air, electrons can transfer out of the SWNTs into an adsorbed water film.

Several studies have observed an abrupt change in sign of the Seebeck coefficient from negative to positive when SWNTs that were previously annealed in vacuum were exposed to air at room temperature (*38*, *39*). These results show a change in the dominant charge carrier from electrons to holes consistent with the electrochemical transfer doping mechanism. Furthermore, small concentrations of gases such as NO_2, NH_3, O_3, and H_2O change the conductivity of SWNTs (*40*–*43*) in the directions predicted by our model.

The electron affinity of a clean GaN surface is reported to be 3.0 ± 0.3 eV (*44*, *45*). Therefore, with a band gap of 3.4 eV, the conduction band minimum is at $E \approx -3$ eV and the valence band maximum is at $E \approx -6.4$ eV. The electrochemical potentials of the oxygen redox couples (−4.83 eV to −5.66 eV) are therefore in the mid-gap region of GaN rather than near the valence band edge as in the case with diamond. Changes in the chemical potential of aqueous redox couples in an adsorbed water film can therefore change the occupancy of the mid-gap surface states that are believed to play a role in the ubiquitous yellow-band emission from GaN. This electrochemical mechanism may be responsible for the enhancement of yellow-band emission in the presence of HCl vapors and diminishment in the presence of NH_3 vapors (*46*, *47*).

Charge transfer between polymers and metals (contact electrification) is a well-known, but not fully understood, phenomenon that depends on the difference in work functions of the contacting materials, presence of surface states, relative humidity, atmospheric adsorbates, humidity, and pH of the ambient environment (*48*, *49*). Sliding friction is another complex phenomenon depending in some situations on the ambient. We suggest that charge transfer to electrochemical acceptors in adsorbed water films may mediate these processes and should be considered when interpreting results. Furthermore, charge transfer to electrochemical acceptors in adsorbed films may influence the properties of nanoparticles and other nanometer-scale structures. This point is of particular interest because the electron energies in small nanopar-

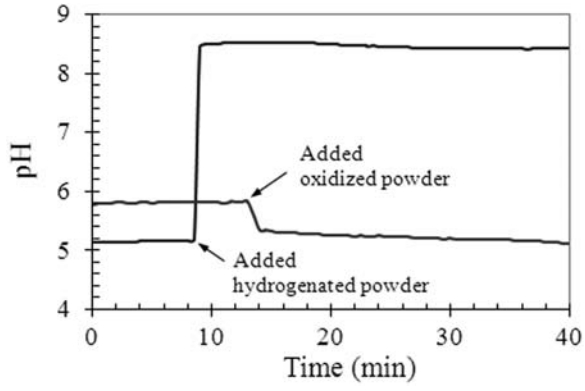

Fig. 6. Changes in pH upon addition of 1 g of hydrogen-terminated natural diamond powder and 1 g of oxidized natural diamond powder, each equilibrated with air, to separate 20-ml solutions with pH ≈ 5. The arrows indicate the point where the diamond powder was added.

ticles will depend on size due to quantum confinement effects.

References and Notes

1. M. I. Landstrass, K. V. Ravi, *Appl. Phys. Lett.* **55**, 975 (1989).
2. R. S. Gi *et al.*, *Jap. J. Appl. Phys. Part 1* **38**, 3492 (1999).
3. K. Hayashi, S. Yamanaka, H. Okushi, K. Kajimura, *Appl. Phys. Lett.* **68**, 376 (1996).
4. H. J. Looi *et al.*, *Diamond Relat. Mater.* **7**, 550 (1998).
5. R. S. Gi *et al.*, *Jap. J. Appl. Phys. Part 1* **36**, 2057 (1997).
6. A. Denisenko, A. Aleksov, E. Kohn, *Diamond Relat. Mater.* **10**, 667 (2001).
7. H. Kawarada, Y. Araki, T. Sakai, T. Ogawa, H. Umezawa, *Phys. Status Solidi* **185**, 79 (2001).
8. K. Hayashi *et al.*, *J. Appl. Phys.* **81**, 744 (1997).
9. T. Maki *et al.*, *Jap. J. Appl. Phys.* **31**, L1446 (1992).
10. F. Maier, M. Riedel, J. Mantel, J. Ristein, L. Ley, *Phys. Rev. Lett.* **85**, 3472 (2000).
11. J. Ristein, M. Riedel, L. Ley, *J. Electrochem. Soc.* **151**, E315 (2004).
12. K. Larsson, J. Ristein, *J. Phys. Chem. B* **109**, 10304 (2005).
13. D. Petrini, K. Larsson, *J. Phys. Chem. C* **111**, 13804 (2007).
14. J. Ristein, *Science* **313**, 1057 (2006).
15. D. Qi *et al.*, *J. Am. Chem. Soc.* **129**, 8084 (2007).
16. A. W. Adamson, *Physical Chemistry of Surfaces* (Wiley, New York, 1982).
17. J. S. Foord *et al.*, *Diamond Relat. Mater.* **11**, 856 (2002).
18. V. Chakrapani, S. C. Eaton, A. B. Anderson, M. Tabib-Azar, J. C. Angus, *Electrochem. Solid-State Lett.* **8**, E4 (2005).
19. A. J. Bard, R. Memming, B. Miller, *Pure Appl. Chem.* **63**, 569 (1991).
20. Yu. Ya. Gurevich, Yu. V. Pleskov, *Elektrokhimiya* **18**, 1477 (1982).
21. *C. R. C. Handbook of Chemistry and Physics*, D. R. Lide, Ed. (CRC Press, Boca Raton, FL, ed. 84, 2003).
22. Yu. V. Pleskov, A. Ya. Sakharova, M. D. Krotova, L. L. Bouilov, B. V. Spitsyn, *J. Electroanal. Chem.* **228**, 19 (1987).
23. G. Piantanida *et al.*, *J. Appl. Phys.* **89**, 8259 (2001).
24. F. Maier, J. Ristein, L. Ley, *Phys. Rev. B* **64**, 165411 (2001).
25. T. N. Rao, D. A. Tryk, K. Hashimoto, A. Fujishima, *J. Electrochem. Soc.* **146**, 680 (1999).
26. J. A. Dean, *Lange's Handbook of Chemistry* (McGraw-Hill, New York, ed. 15, 1999).
27. B. Rezek *et al.*, *Appl. Phys. Lett.* **82**, 2266 (2003).
28. P. C. Hiemenz, R. Rajagopalan, *Principles of Colloid and Surface Chemistry* (Dekker, New York, ed. 3, 1997).
29. A. W. Neumann, R. J. Good, *Techniques of Measuring Contact Angles, Surface and Colloid Science*, vol. II, *Experimental Methods*, R. J. Good, R. R. Stromberg, Eds. (Plenum, New York, 1979).
30. N. Matsuka, Y. Nakagawa, M. Kurihara, T. Tonomura, *Desalination* **51**, 163 (1984).
31. G. S. Woods, in *Properties and Growth of Diamond*, G. Davies, Ed. (EMIS Datareviews Ser. 9, Institution of Chemical Engineers, London, 1994), pp. 83–84.
32. T. Evans, in *The Properties of Natural and Synthetic Diamond*, J .E. Field, Ed. (Academic Press, London, 1992), p. 239.
33. A. T. Collins, E. C. Lightowlers, in *Properties of Diamond*, J. E. Field, Ed. (Academic Press, London, 1979), p. 99.
34. J. Ristein, M. Reidel, M. Stammler, B. F. Mantel, L. Ley, *Diamond Relat. Mater.* **11**, 350 (2002).
35. S. Kazaoui, N. Minami, N. Matsuda, H. Kataura, Y. Achiba, *Appl. Phys. Lett.* **78**, 3433 (2001).
36. J. Zhao, J. Han, J. Lu, *Phys. Rev. B* **65**, 1934011 (2002).
37. D. Lovall, M. Buss, E. Graugnard, R. P. Andres, R. Reifenberger, *Phys. Rev. B* **61**, 5683 (2000).
38. K. Bradley *et al.*, *Phys. Rev. Lett.* **85**, 4361 (2000).
39. G. U. Sumanasekera, C. K. W. Adu, S. Fang, P. C. Eklund, *Phys. Rev. Lett.* **85**, 1096 (2000).
40. P. G. Collins, K. Bradley, M. Ishigami, A. Zettl, *Science* **287**, 1801 (2000).
41. J. Kong *et al.*, *Science* **287**, 622 (2000).
42. S. Picozzi *et al.*, *J. Vac. Sci. Technol. A* **22**, 1466 (2004).
43. A. Zahab, L. Spina, P. Poncharal, C. Marlieri, *Phys. Rev. B* **62**, 10000 (2000).
44. K. M. Tracy, P. J. Hartlieb, R. F. Davis, E. H. Hurt, R. J. Nemanich, *J. Appl. Phys.* **94**, 3939 (2003).
45. V. M. Bermudez, *J. Appl. Phys.* **80**, 1190 (1996).
46. V. Chakrapani, thesis, Case Western Reserve University, Cleveland, OH (2007).
47. V. Chakrapani, J. C. Angus, A. B. Anderson, G. Sumanasekera, *Mater. Res. Soc. Symp. Proc.* **956,** paper 0956-J15-01 (2007)
48. J. A. Wiles, M. Fialkowski, M. R. Radowski, G. M. Whitesides, B. A. Grzybowski, *J. Phys. Chem. B* **108**, 20296 (2004).
49. S. Trigwell, N. Grable, C. U. Yurteri, R. Sharma, M. K. Mazumder, *IEEE Trans. Ind. Appl.* **39**, 79 (2003).

50. We thank J. Adin Mann and D. J. Lacks for useful discussions. C. C. Hayman provided invaluable experimental support. Financial support of the NSF (grant CHEM 0314688) and Case Western Reserve University is gratefully acknowledged.

6 August 2007; accepted 16 October 2007
10.1126/science.1148841

REPORTS

Coherent Control of a Single Electron Spin with Electric Fields

K. C. Nowack,*† F. H. L. Koppens,† Yu. V. Nazarov, L. M. K. Vandersypen*

Manipulation of single spins is essential for spin-based quantum information processing. Electrical control instead of magnetic control is particularly appealing for this purpose, because electric fields are easy to generate locally on-chip. We experimentally realized coherent control of a single-electron spin in a quantum dot using an oscillating electric field generated by a local gate. The electric field induced coherent transitions (Rabi oscillations) between spin-up and spin-down with 90° rotations as fast as ~55 nanoseconds. Our analysis indicated that the electrically induced spin transitions were mediated by the spin-orbit interaction. Taken together with the recently demonstrated coherent exchange of two neighboring spins, our results establish the feasibility of fully electrical manipulation of spin qubits.

Spintronics and spin-based quantum information processing provide the possibility of adding new functionality to today's electronic devices by using the electron spin in addition to the electric charge (*1*). In this context, a key element is the ability to induce transitions between the spin-up and spin-down states of a localized electron spin and to prepare arbitrary superpositions of these two basis states. This is commonly accomplished by magnetic resonance, whereby bursts of a resonant oscillating magnetic field are applied (*2*). However, producing strong oscillating magnetic fields in a semiconductor device requires specially designed microwave cavities (*3*) or microfabricated striplines (*4*), and this has proven to be challenging. In comparison, electric fields can be generated much more easily, simply by exciting a local gate electrode. In addition, this allows for greater spatial selectivity, which is important for local addressing of individual spins. It would thus be highly desirable to control the spin by means of electric fields.

Although electric fields do not couple directly to the electron spin, indirect coupling can still be realized by placing the spin in a magnetic field gradient (*5*) or in a structure with a spatially varying g tensor, or simply through spin-orbit interaction, present in most semiconductor structures (*6*, *7*). Several of these mechanisms have been used to electrically manipulate electron spins in two-dimensional electron systems (*8*–*11*), but proposals for coherent electrical control at the level of a single spin (*5*, *12*–*15*) have so far remained unrealized.

We demonstrate coherent single spin rotations induced by an oscillating electric field. The electron is confined in a gate-defined quantum dot (Fig. 1A), and we use an adjacent quantum dot, containing one electron as well, for readout. The ac electric field is generated through excitation of one of the gates that form the dot, thereby

Kavli Institute of Nanoscience, Delft University of Technology, Post Office Box 5046, 2600 GA Delft, the Netherlands.

*To whom correspondence should be addressed. E-mail: k.c.nowack@tudelft.nl, l.m.k.vandersypen@tudelft.nl
†These authors contributed equally to this work.